Eur. Phys. J. D **17**, 167–173 (2001)

THE EUROPEAN PHYSICAL JOURNAL D

EDP Sciences

High accuracy Dirac-finite-element (FEM) calculations for H_2^+ and Th_2^{179+}

O. Kullie[a] and D. Kolb [b]

Physics Department, University of Kassel, 34132 Kassel, Germany

Received 16 February 2001 and Received in final form 12 July 2001

Abstract. A two-dimensional, fully numerical approach to the four-component first-order Dirac-differential-equation utilizing the Finite-Element-Method (FEM) is employed for H_2^+ and Th_2^{179+}. Using elliptic-hyperbolic coordinates and further one-dimensional singular transformations, scaling transformations and extrapolation techniques (geometrical over iteration steps and logarithmic over grid points) we achieve for the molecules H_2^+ and Th_2^{179+} relative accuracies better than 10^{-12} for $1(1/2)g$ energies.

PACS. 02.70.Dh Finite-element and Galerkin methods – 03.65.Ge Solutions of wave equations: bound states – 31.15.Ar Ab initio calculations

1 Introduction and method

The methods for the fully numerical treatment of diatomic molecules, which have been established over more than a decade, are the Finite-Difference-Method (FDM) [1] and the Finite-Element-Method (FEM) [2–10]. For a given number of node points the results achieved by the FEM were always more accurate than those with the FDM. The FEM was extended from the solution of the Schrödinger-equation for H_2^+ [2], to the solution of the Hartree-Fock-Slater- [3], Hartree-Fock- [4], Dirac- [5], Dirac-Fock-Slater- [6,7] and Dirac-Fock- [10] equations for diatomic molecules. In [7,8] it was shown, that the Finite-Element-Method is able to provide very accurate solutions of the two-center Dirac-equation for very small molecules and very heavy quasi-molecules. In the present letter the first order Dirac-differential-equations are solved highly accurately numerically for H_2^+ and Th_2^{179+}, using the Finite-Element-Method (FEM). The energies may be used as benchmarks *e.g.* in molecular relativistic calculations for calibrating basis sets. The main purpose of this paper however was to investigate the convergence behavior of relativistic solutions and develop strategies for FEM approximations with high efficiency (accuracy *vs.* computational effort) without the need for extended precision computation. The relativistic Dirac-Hamilton operator for one electron molecules is defined as:

$$\hat{H} = c\hat{\alpha}\cdot\hat{\mathbf{p}} + mc^2\hat{\beta} - \sum_{k=1}^{K}\frac{e^2 Z_k}{|\mathbf{r}-\mathbf{R}_k|} \qquad (1)$$

with $\hat{\alpha}$ and $\hat{\beta}$ being the Dirac matrices, and K the number of atoms.
In order to get the Dirac-equation we used the single particle energy functional

$$I = \langle\psi \mid \hat{H} - \varepsilon \mid \psi\rangle\cdot \qquad (2)$$

The total energy is given by:

$$E_{\rm tot} = \varepsilon + E_{\rm nuc}, \quad \text{where} \quad E_{\rm nuc} = \frac{e^2 Z_1 Z_2}{R}\cdot \qquad (3)$$

As advantageous for two-center Coulombic problems we describe them in elliptic hyperbolic coordinates ξ and η

$$x = \frac{R}{2}u(\xi,\eta)\,\cos(\varphi), \quad y = \frac{R}{2}u(\xi,\eta)\,\sin(\varphi), \quad z = \frac{R}{2}\xi\eta \qquad (4)$$

where $u(\xi,\eta) = \sqrt{(\xi^2-1)(1-\eta^2)}$ and R is the internuclear distance. The Coulomb singularity of point nuclei causes a singular behavior of the solution at the nuclei of the form $r_i^{-1+\gamma_{l,k}}$, well known from atomic calculations. Thus further singular coordinate transformations (the back transform is non analytic) are needed (see Appendix A)

$$\xi = 1 + c_1\sinh^m(s/2) + c_2\sinh^{(m+2)}(s/2) + ...; \qquad 0 \le s < \infty \qquad (5)$$

$$\eta = 1 - c_1\sin^m(s/2) + c_2\sin^{(m+2)}(s/2) + ...; \qquad 0 \le t \le \pi \qquad (6)$$

$$\text{for } m = 2,4,6,8,10, \text{ with } c_i = 0 \quad \text{for} \quad i > \frac{m}{2}\cdot$$

[a] e-mail: kullie@hrz.uni-kassel.de
[b] e-mail: kolb@physik.uni-kassel.de

The standard regularization of relativistic problems by the transformation $r = \exp(x)$ (r = radial space coordinate, x = intrinsic coordinate) maps the interval $[0, \infty)$ to $(-\infty, \infty)$ and regularizes to infinite order. Thus one is overdoing the needs of finite numerics, the price being large numbers of needed grid points. Our transformations keep the intervals and only partially regularize the singular behavior of the solution at the nuclei, but already allow higher convergence orders depending on m, see Tables 5–9. Singular transformations of the type $\lim_{s\to 0} \xi - 1 \sim s^4$ and $\lim_{t\to 0,\pi} 1 - \eta \sim t^4$ have already successfully been used before [5–7], but in contrast to equations (5, 6) they violated the symmetry that ξ, η are equivalent parabolic coordinates for $s, t \to 0$. This lead to accuracies inferior to the present ones, and did not exhibit clear extrapolation properties. Because of axial symmetry the angular coordinate φ is treated analytically by the Ansatz [11]

$$\psi = \begin{pmatrix} \psi^L(s,t,\varphi) \\ \psi^S(s,t,\varphi) \end{pmatrix} = \begin{pmatrix} \phi^1(s,t)\, \mathrm{e}^{\mathrm{i}(j_z - 1/2)\varphi} \\ \phi^2(s,t)\, \mathrm{e}^{\mathrm{i}(j_z + 1/2)\varphi} \\ \mathrm{i}\phi^3(s,t)\, \mathrm{e}^{\mathrm{i}(j_z - 1/2)\varphi} \\ \mathrm{i}\phi^4(s,t)\, \mathrm{e}^{\mathrm{i}(j_z + 1/2)\varphi} \end{pmatrix} \tag{7}$$

for the four component spinor of a single electron wave function ψ. Here $j_z = \langle j_z \rangle$ describes the projection of the total angular momentum onto the inter-nuclear axis. The spinor wave functions ϕ^k are expanded in terms of the global functions $G^k(s,t) = G_1^k(s,t)\, G_2(s,t)$, which are defined over all elements, and shape-functions $N_j(s,t)$, which are defined on each element [5]

$$\begin{aligned} \phi^k(s,t) &= G^k(s,t) \sum_j u_j^k N_j(s,t) \\ &= G_1^k(s,t)\, G_2(s,t) \sum_j u_j^k N_j(s,t) \end{aligned} \tag{8}$$

$$\begin{aligned} G_1^k(s,t) &= \left[(\xi^2 - 1)(1 - \eta^2)\right]^{\frac{(j_z \pm \frac{1}{2})}{2}}, \\ &\text{with ``–'' for } k = 1,3 \text{ and ``+'' for } k = 2,4, \\ \text{and } G_2(s,t) &= r_1^{-1+\gamma_{1,\kappa}} r_2^{-1+\gamma_{2,\kappa}}, \\ \gamma_{l,\kappa} &= \sqrt{\kappa^2 - \left(\frac{Z_l}{c}\right)^2},\ \kappa = |j_z| + \frac{1}{2},\ l = 1,2 \end{aligned} \tag{9}$$

where l denotes the left, and right center respectively. $N_j(s,t)$ are complete polynomials of order p in s, t, but transcendental functions in ξ, η. Expansion (8) is inserted into functional (2). In order to find the stationary value of functional (2), it is differentiated with respect to the coefficients u_j^k. In contrast to previous works we used an open boundary at $s = s_{\max}$ and also at the symmetry axis $s = 0, t = 0, \pi$. This leads especially near the outer boundary ($s = s_{\max}$) to an oscillatory behavior of the solutions, but stays sufficiently small for higher numbers of grid points and a slightly increased solution domain compared to non-relativistic FEM calculations of similar quality. A better treatment from an analytical point of view of the boundary conditions by variation of the values at the boundary has not been investigated yet, because this would constitute a non-linear problem to be solved by additional iterations. Besides increasing the complexity of the calculations this might become a source of instabilities. Finally we are led to a matrix eigenvalue problem with a $4N \times 4N$ symmetric matrices:

$$(\mathbf{H} - \varepsilon \mathbf{S})\, u_i = 0 \tag{10}$$

where N is the number of grid points used for the discretization. The matrix $\mathbf{H}$ results from the first term of the functional (2) and the matrix $\mathbf{S}$ from the second term. Due to the local character of the shape-functions $N_j(s,t)$ which are only defined on one element the matrices $\mathbf{H}$ and $\mathbf{S}$ are very sparse. The sparseness is only partially exploited (hull of the matrix) as we solve the matrix equation (10) by a Cholesky decomposition and inverse vector iteration. Thus the computer effort scales quadratically with N.

2 Results and discussion

In Tables 1 and 2 we present the energies of the $1(1/2)g$ for the H_2^+, Th_2^{179+} molecules at an inter-nuclear distance $R = 2$, $R = 2/90$ a.u. respectively. In all our calculations we set the speed of light to be $1/\alpha = 137.0359895$. The two tables show the behavior of the energy error of the first $(1/2)g$ state depending on the number of finite elements and the number of given node points. Tables 1 and 2 were performed with 5th order polynomials and $m = 4$ for H_2^+ and 7th order polynomials with $m = 6$ for Th_2^{179+}. Bold digits don't change any more when increasing the number of node points. The radial dimension extended to 26 a.u. for H_2^+, and 0.14 a.u. for Th_2^{179+}. Relative accuracies better than 1×10^{-12} for the first 1/2 state have been achieved. Further calculations with different FEM orders and various m are shown in Tables 5–9.

For regular subdivisions and a sufficiently smooth solutions, with the diameter of the elements proportional to the root of N, the asymptotic convergence behavior (N towards infinity) for a 2-dimensional finite element method is known as[1]

$$E_{\inf} - E_N = \Delta E(N) \le C\, N^{-q} \tag{11}$$

where $E_{\inf}$ is the true value [12,13]. C may be determined from two calculations with a differently large number of grid points. For the singular Dirac-solutions an asymptotic error of the type equation (11) may still hold, but it depends on the amount of partial regularization (given by m) whether q is dominated by the FEM error ($q = 2p$ for linear elements ($p = 1$), and $q = p$ otherwise, m sufficiently large), or rather by the singular factor $\gamma_{l,k}$. Since $\gamma_{l,k}$ for H_2^+ is almost 1, one more or less finds $q = 2p, q = p$ respectively. But for Th_2^{179+} $\gamma_{l,k}$ is such that convergence factors are close to multiples of half integers. For the asymptotic expansion one therefore should use two mixed forms:

[1] For first order FEM $q = 2p$, for higher order $q = p$, where p is the FEM order.

Table 1. $1(1/2)g$ energies for H_2^+ at $R = 2$ a.u., $s_{\max} = 26$ a.u., $m = 4$, 5th order FEM, all values in a.u.

Elements / Points (N)	$\varepsilon_{1(1/2)g}$	$\varepsilon^{\infty}_{1(1/2)g}$ [1]
32 / 441	**−1.10264**95743536	**−1.10264**614727131
72 / 961	**−1.10264**18094468	**−1.10264**180213691
128 / 1 681	**−1.1026415**809214	**−1.1026415**8404107
200 / 2 601	**−1.1026415**809207	**−1.1026415**8123017
288 / 3 721	**−1.1026415**808935	**−1.1026415**8091607
392 / 5 041	**−1.1026415810**126	**−1.1026415810**2510
512 / 6 561	**−1.1026415810**142	**−1.1026415810**3099
648 / 8 281	**−1.10264158103**20	**−1.10264158103**27
800 / 10 201	**−1.10264158103**270	**−1.102641581033**498
968 / 12 321	**−1.10264158103**164	**−1.102641581033**555
extrapol. value [2]		**−1.1026415810335**80

[1] Geometrically extrapolated values over iteration steps ($\to \infty$).
[2] Logarithmically extrapolated values over effective number of grid points ($N^* \to \infty$), where $N^* = (N_s - 1)\,(N_t - 1)$, where $N_{s,t}$ are number of the grid points in s, t direction respectively.

Table 2. $1(1/2)g$ energies for Th_2^{179+} at $R = 2/90$ a.u., $s_{\max} = 0.14$ a.u., $m = 8$, 7th order FEM, all values in a.u., see Table 1.

Elements / Points (N)	$\varepsilon_{1(1/2)g}$	$\varepsilon^{\infty}_{1(1/2)g}$ [1]
32 / 841	**−9 504.**8244669286	**−9 504.7**8244670023
72 / 1 849	**−9 504.756**6906673	**−9 504.756**96913949
128 / 3 249	**−9 504.7567**523556	**−9 504.75675**234274
200 / 5 041	**−9 504.7567471**712	**−9 504.75674**715109
288 / 7 225	**−9 504.7567469**478	**−9 504.756746**94615
392 / 9 801	**−9 504.75676926**377	**−9 504.7567469**26250
512 / 12 769	**−9 504.75676935**510	**−9 504.75674692**35527
extrapol. value [2]		**−9504.75674692**29

[1] Geometrically extrapolated values over iteration steps ($\to \infty$).
[2] Logarithmically extrapolated values over effective number of grid points ($N^* \to \infty$), where $N^* = (N_s - 1)\,(N_t - 1)$, where $N_{s,t}$ are number of the grid points in s, t direction respectively.

one for integer q stemming from the FEM asymptotic expansion of the smooth part and one with real q as the leading term to extrapolate the singular contributions. As there are usually not enough values of different numbers of node points available to make such a complex extrapolation we used the fact that for certain m (*e.g.* $m = 4$) the leading singular power is close to an integer for Th_2^{179+} also. Thus the two errors may reasonably well be combined into one asymptotic expansion; one asymptotic expansion up to a certain order in $1/N$ also holds for $q \ll p$ or $p \ll q$. The fact that we do have a unique scale in our 2-dimensional calculations comes from an equidistant subdivision in the intrinsic coordinates s, t with the same numbers of node points $N_s = N_t$. Thus the scales are connected $h_s = \text{const.} \times h_t$ with a constant factor independent of $N, h_s = s_{\max}/(N_s - 1), h_t = \pi/(N_t - 1)$. So we did the extrapolation with respect to the effective number of grid points $N^* = (N_s - 1)(N_t - 1)$.

Equation (11) as an asymptotic relation holds only approximately for finite N. From three calculations with different numbers of node points one may test how well the (asymptotic) equation (11) is satisfied.

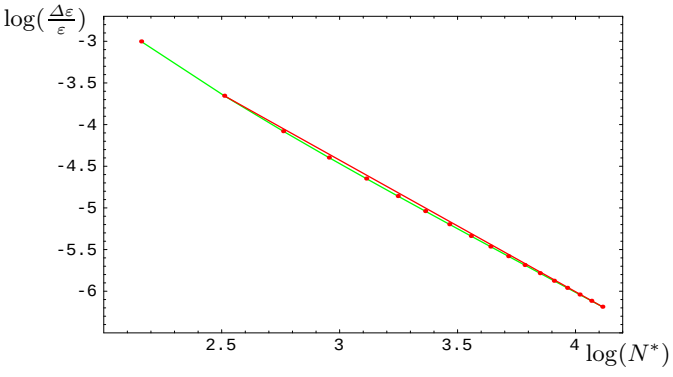

Fig. 1. Th_2^{179+}, $\log(\Delta\varepsilon/\varepsilon)$ *vs.* $\log(N^*)$, $m = 2$, 3rd order FEM.

For the reasonably large numbers N employed in this paper it holds already with good accuracy, as seen in Figure 1, where we plot $\Delta\varepsilon/\varepsilon$ (geometrically extrapolated

Table 3. H_2^+ convergence order q, geometrically extrapolated values used.

Order/Coord.	$m=2$	$m=4$	$m=6$	$m=8$
1	2	2	2	2
3	3	3	3[a]	
5	3	5[a]	5[a]	

[a] not clearly exhibited.

Table 4. Th_2^{179+} convergence order q, see Table 3.

Order/Coord.	$m=2$	$m=4$	$m=6$	$m=8$	$m=10$
1	1.5	2	2		
3	1.5	3	3		
5	1.5	3	4.5[a]		
7	1.5	3	4.5	6[a]	7

values) *versus* the effective number of grid points N^* in a doubly logarithmic diagram. The slope of the straight line gives the exponent of the power law which is the convergence order. Tables 3 and 4 show this convergence behavior for various m and various FEM orders for the molecules H_2^+, Th_2^{179+} respectively. It is obvious from the tables that only if the coordinate transformation allows it, *i.e.* the singularity is partially regularized to sufficiently high order, the full convergence order of FEM can be exploited. Then from equation (11) one expects the slope to be[2] 2 for linear elements and p (the FEM order) for higher order of elements. More accurately extrapolated values are obtained due to the logarithmic asymptotic expansions of the energy error by inverse powers or rational functions [14–17]. Extrapolation over the iteration number was done by geometric asymptotic expansions [14,15]. In the Tables 1, 2 and 5–9 extrapolation over grid points done with respect to N^*, the effective number of grid points. We found rational extrapolations to be more stable than inverse powers, so we used them throughout. Values up to the number of points displayed in the first column were included in the logarithmic extrapolation, q was taken from Tables 3 and 4 for H_2^+ and Th_2^{179+} respectively. Underlined digits are gained by extrapolation.

In Figure 2 the upper group of lines represent geometrically extrapolated direct calculated values, the lower group of lines are in addition logarithmically extrapolated over the grid points up to the various maximal effective numbers of points N^* displayed. Figures 2 and 3 (see also Tabs. 5 and 7) show values of first order calculations for various m, geometrically and logarithmically extrapolated. We see in the diagrams how extrapolation behaves, when the singularity is partially regularized: for $m > 2$, it is efficient. Figure 4 (see also Tab. 8) shows that extrapolation can better work when the coordinate transformations and the FEM order are suitably chosen. For Th_2^{179+}, $m = 8$ with 1st order FEM[3] and $m = 6$ with 3rd order FEM and $m = 6, 8$ with 7th order FEM (see Tab. 9) give

[2] See discussion of equation (11).

[3] Very poor extrapolation gains as in non-rel. calculation of [14].

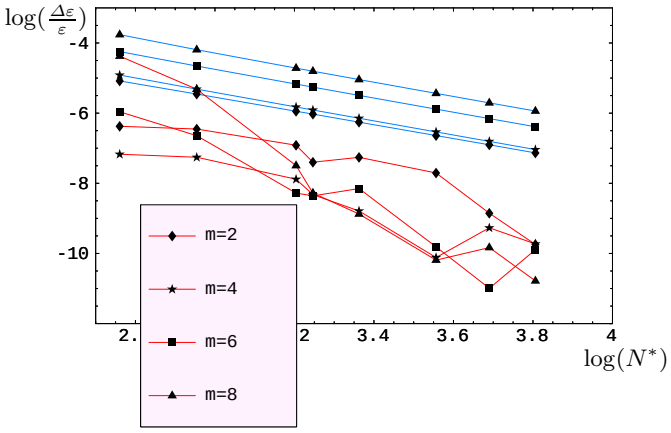

Fig. 2. H_2^+, $\log(\Delta\varepsilon/\varepsilon)$ *vs.* $\log(N^*)$, $m = 2, 4, 6, 8$, 1st order FEM, $N^*_{\max} = 6\,400$, see text. The extrapolated values are from Table 5.

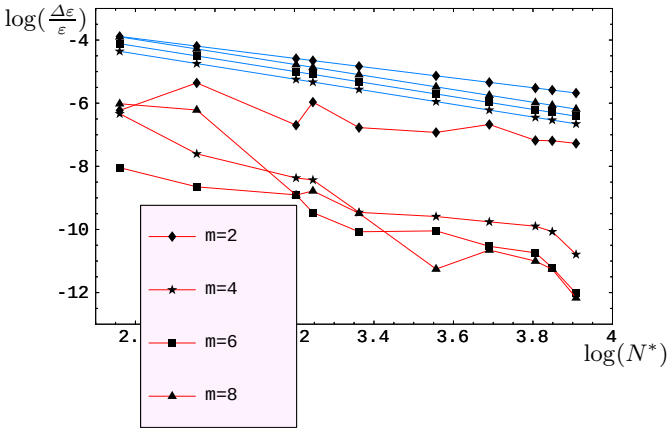

Fig. 3. Th_2^{179+} $\log(\Delta\varepsilon/\varepsilon)$ *vs.* $\log(N^*)$, $m = 2, 4, 6, 8$, 1st order FEM, $N^*_{\max} = 8\,100$, see text. The extrapolated values are from Table 7.

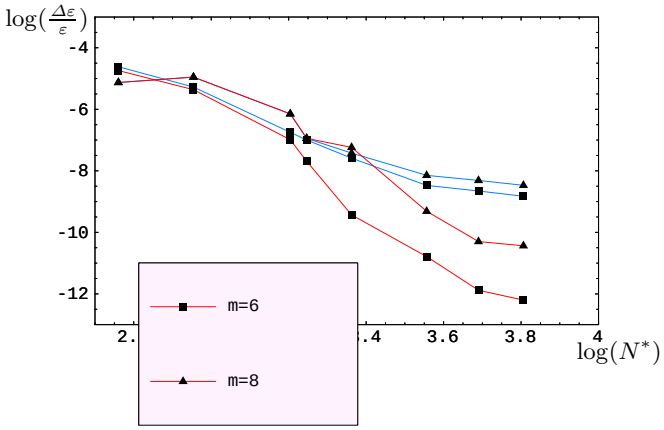

Fig. 4. Th_2^{179+} $\log(\Delta\varepsilon/\varepsilon)$ *vs.* $\log(N^*)$, $m = 6, 8$, 3rd order FEM, $N^*_{\max} = 9\,216$, see text. The extrapolated values are from Table 8.

Table 5. H_2^+ $\varepsilon_{1(1/2)g}$ values extrapolated over effective number of grid points N^*, 1st order FEM and various coordinate transformations. Underlined digits are gained by extrapolation.

N^*	$m=2$	$m=4$	$m=6$	$m=8$
576	**−1.10264**111553	**−1.10264**150667	**−1.10264**278450	**−1.1026**8810614
900	**−1.10264**196950	**−1.10264**164198	**−1.10264**183213	**−1.10264**687519
1 600	**−1.10264**144692	**−1.10264**156664	**−1.10264158**686	**−1.10264**161626
1 764	**−1.10264**162507	**−1.10264158**627	**−1.10264**157623	**−1.10264158**861
2 304	**−1.1026415**2046	**−1.10264**157926	**−1.10264**157326	**−1.10264**157959
3 600	**−1.10264**155934	**−1.10264158**114	**−1.10264158**089	**−1.10264158**114
4 900	**−1.10264**157951	**−1.10264158**165	**−1.10264158**106	**−1.10264158**011
6 400	**−1.10264158**086	**−1.10264158**085	**−1.10264158**120	**−1.10264158**107
	−1.10264166215[d]	**−1.10264**148020[d]	**−1.10264**117296[d]	**−1.1026**4043678[d]

[d] geometrically extrapolated direct calculated values for last N^*.

Table 6. H_2^+ $\varepsilon_{1(1/2)g}$ values, 5th order FEM, see Table 5.

N^*	$m=2$	$m=4$	$m=6$
900	**−1.10264**2736780	**−1.10264**1719249	**−1.1026**38899885
1 600	**−1.10264**1722561	**−1.10264**15699941	**−1.10264**1504321
3 600	**−1.10264158**3963	**−1.10264158**08578	**−1.10264**162509
4 900	**−1.10264158**1697	**−1.1026415810**399	**−1.10264158**2108
8 100	**−1.10264158**1188	**−1.1026415810**325	**−1.1026415810**08
10 000	**−1.10264158**1000	**−1.1026415810**337	**−1.1026415810**56
12 100	**−1.10264158**10450	**−1.10264158103358**0	**−1.1026415810**324
	−1.1026415816748[d]	**−1.10264158103**355[d]	**−1.1026415810**312[d]

Table 7. Th_2^{179+} $\varepsilon_{1(1/2)g}$ values, 1st order FEM, see Table 5.

N^*	$m=2$	$m=4$	$m=6$	$m=8$
576	**−9 504.75**114623	**−9 504.75**233313	**−9 504.756**83307	**−9 504.7**65865
900	**−9 504.7**1502758	**−9 504.756**51064	**−9 504.756**66472	**−9 504.75**096721
1 600	**−9 504.75**866813	**−9 504.7567**0619	**−9 504.7567**5875	**−9 504.7567**5855
1 760	**−9 504.7**4644564	**−9 504.7567**8214	**−9 504.75674**367	**−9 504.7567**3113
2 304	**−9 504.75**835048	**−9 504.75674**361	**−9 504.75674**772	**−9 504.7567**5001
3 600	**−9 504.75**787360	**−9 504.75674**937	**−9 504.75674**606	**−9 504.756746**87
4 900	**−9 504.75**473381	**−9 504.75674**858	**−9 504.756746**64	**−9 504.75674**713
6 400	**−9 504.75**737659	**−9 504.75674**571	**−9 504.756746**75	**−9 504.75674**701
7 056	**−9 504.75**558213	**−9 504.756746**11	**−9 504.75674**716	**−9 504.7567469**75
	−9 504.77675486[d]	**−9 504.75**952087[d]	**−9 504.7**6159261[d]	**−9 504.7**64892757[d]

Table 8. Th_2^{179+} $\varepsilon_{1(1/2)g}$ values, 3rd order FEM, see Table 5.

N^*	$m=2$	$m=4$	$m=6$	$m=8$
576	**−9 504.**67010417	**−9 504.7**1199453	**−9 504.9**296417	**−9 504.**68598090
900	**−9 504.7**5529360	**−9 504.756**51005	**−9 504.7**1549429	**−9 504.**86264417
1 764	**−9 504.756**28204	**−9 504.7567**3691	**−9 504.7**577209	**−9 504.7**6349584
2 304	**−9 504.756**52589	**−9 504.7567**6551	**−9 504.756**94084	**−9 504.75**566638
3 600	**−9 504.756**53871	**−9 504.75674**757	**−9 504.75675**043	**−9 504.75**729697
7 056	**−9 504.7567**0829	**−9 504.756746**34	**−9 504.75674**707	**−9 504.75674**232
8 100	**−9 504.7567**5565	**−9 504.75674**707	**−9 504.756746**91	**−9 504.75674**228
9 216	**−9 504.7567**1753	**−9 504.7567469**17	**−9 504.75674692**0	**−9 504.756746**575
	−9 504.76717904[d]	**−9 504.7567**6014[d]	**−9 504.7567**6110[d]	**−9 504.75677**907[d]

Table 9. Th_2^{179+} $\varepsilon_{1(1/2)g}$ values, 7th order FEM, see also Table 5.

N^*	$m = 4$	$m = 6$	$m = 8$
784	**−9 504.777**163068	**−9 504.756**481450	
1 764	**−9 504.7567**779596	**−9 504.756727**202	**−9 504.7567**77125
4 900	**−9 504.756746**735	**−9 504.75674691**3	**−9 504.756746**770
7 056	**−9 504.756746**861	**−9 504.756746922**3	**−9 504.75674692**1
9 604	**−9 504.756746915**	**−9 504.7567469224**	**−9 504.75674692279**
12,544	**−9 504.75674692**3	**−9 504.756746921**0	**−9 504.75674692**29
	−9 504.7567497462[d]	**−9 504.75674692**8[d]	**−9 504.75674692**35[d]

Table 10. Comparison of the $\epsilon_1(1/2)g$ energies with literature values.

Sp. of light	Th_2^{179+}		H_2^+	
137.0359895	**−9 504.756746923**		**−1.10264158103358**	
137.0359895	−9 504.7567155	[22]	−1.102641579334[1]	[21]
137.03602	−9498.98	[23]	−1.102565	[23]
137.0359895	−9 504.756696	[24]	−1.1026415801	[24]
	−9 504.7497	[25]	−1.102481	[26]
	−9 504.7567151[2]	[18]		

[1] This value results from adding their $\Delta E_{\text{rel.}}$ to their $E^0_{\text{nrel.}}$ (non-rel. value); one notes however that their $\Delta E_{\text{rel.}}$ is more accurate and reaches almost the corresponding FEM value [5].
[2] Solution od Dirac-eq. based on the Bloch equation of DPT.

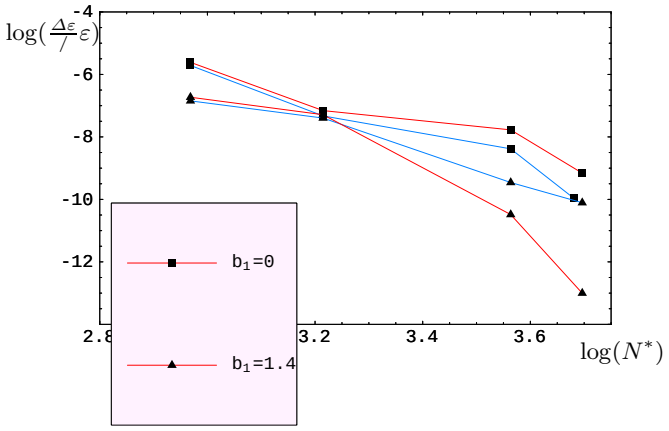

Fig. 5. H_2^+ $\log(\Delta\varepsilon/\varepsilon)$ *vs.* $\log(N^*)$, $m = 6$, 5th order FEM, $N^*_{\max} = 4\,970$. Parameter $b_1 = 0$ (no scaling, logarithm. extrap. values are from Tab. 6), and $b_1 = 1.4$. For the same b_1 the upper line connects geometrically extrapolated values, and the lower line connects values, which logarithmically extrapolated in addition.

the best values after extrapolation. For H_2^+, $m = 4$ with 5th order FEM gives the best results; extrapolation in this case can only slightly improve them as one notices from Table 1[4].

[4] The improvement is only for large grid point numbers, the effect of geometrical and logarithmic extrapolation are seen in Tables 1 and 6 for $m = 4$.

Scaling transformation

We have seen that the singular coordinate transformation equations (5, 6) can partially regularize the singularity at the nuclei and thus allow high convergence orders. But they affect the element density far away from the singular point and make this area sparse. The scaling transformation (see Appendix A.2) varies the element density and may raise it in the distant regions but still remains linear in the neighborhood of the singularity. The effect on the obtained accuracy is displayed for H_2^+ in Figure 5. There we compare a 5th order calculation for singular transformation $m = 6$, with $b_1 = 0$ (no scaling, see Tabs. 1 and 6), and with $b_1 = 1.4$, for the scaling transformation parameter. We display extrapolated and non-extrapolated values. One reaches a higher accuracy for the same number of grid points N; conversely for the same accuracy one needs a smaller number of grid points, and thus less computational effort.

3 Conclusion

We presented highly accurate FEM solutions of the molecular one-electron Dirac-equation for a very light system H_2^+ and a very heavy system Th_2^{179+} thus spanning the full range from quite non-relativistic to highly relativistic quasi-molecules. Comparing the non-relativistic FEM-solutions of the one electron Schrödinger-equation, 2 to 3 times more points are needed here in the relativistic case for comparable accuracies. Despite the dramatic improvements in efficiency (accuracy *vs.* effort) of the presented calculations, techniques scaling linear with the number of variables for the solutions of the FEM matrix

equations, *e.g.* FEM multi-grid, as in non-relativistic FEM applications already successfully employed [20] should further strongly reduce the present computer effort. This is needed to overcome the still unsatisfactory high computer time and storage requirements of present relativistic FEM calculations, scaling with N^2. It has been already shown [9] that a relativistic LCAO defect correction scheme (LCAO-DKM) may give a considerable improved accuracy for the same number of FEM-grid points (unknowns) and thus allows for further efficiency gains. These efficiency considerations do not prevent highly accurate benchmark values, but they limit the size of the electronic systems calculable with reasonable computer resources. Very attractive are alternative 2-spinor variationally bound formulations of the relativistic one-electron problem [18,19]. *E.g.* in [18] a rather high accuracy in a Gaussian basis for Th_2^{179+} has been achieved. Besides reducing the number of unknowns by a factor of 2 their analogy to non-relativistic formulations should give the fast multi-grid method for the solution of the FEM matrix equations about the same efficiency as in truly non-relativistic applications [20].

This work was partially supported by the Deutsche Forschungsgemeinschaft (DFG).

Appendix A: Coordinate transformations

The following coordinate transformations are employed.

A.1 Singular transformations

$$
\begin{aligned}
m=2\text{: } \xi &= 1+2\sinh^2(s/2)=\cosh(s),\\
\eta &= 1-2\sin^2(t/2)=\cos(t)\\
m=4\text{: } \xi &= 1+6\sinh^4(s/2)+4\sinh^6(s/2)\\
\eta &= 1-6\sin^4(t/2)+4\sin^6(t/2)\\
m=6\text{: } \xi &= 1+20\sinh^6(s/2)+30\sinh^8(s/2)+12\sinh^{10}(s/2)\\
\eta &= 1-20\sin^6(t/2)+30\sin^8(t/2)-12\sin^{10}(t/2)\\
m=8\text{: } \xi &= 1+70\sinh^8(s/2)+168\sinh^{10}(s/2)\\
&\quad +140\sinh^{12}(s/2)+40\sinh^{14}(s/2)\\
\eta &= 1-70\sin^8(t/2)+168\sin^{10}(t/2)\\
&\quad -140\sin^{12}(t/2)+40\sin^{14}(t/2)\\
m=10\text{: } \xi &= 1+252\sinh^{10}(s/2)+840\sinh^{12}(s/2)\\
&\quad +1080\sinh^{14}(s/2)+630\sinh^{16}(s/2)\\
&\quad +140\sinh^{18}(s/2)\\
\eta &= 1-252\sin^{10}(t/2)+840\sin^{12}(t/2)\\
&\quad -1080\sin^{14}(t/2)+630\sin^{16}(t/2)-140\sin^{18}(t/2)\\
\text{where}\quad & 0\le s<\infty;\ \le t\le\pi.
\end{aligned}
$$

They have the following simple derivative forms[5]:

$$\mathrm{d}\xi/\mathrm{d}s = D_m\,\sinh^{m-1}(s),\quad \mathrm{d}\eta/\mathrm{d}t = D_m\,\sin^{m-1}(t).$$

[5] One can integrate the forms, with Mathematica for example, to see that these transformation are connect to the hyper geometrical function 2F1, and after some manipulations one become the coordinate transformations for the varies m.

A.2 Scaling transformations

$$
\begin{aligned}
S &= s_{\max}\left[\frac{\sinh(b_1\,s)}{\tanh(b_1\,s_{\max})}-2\sinh^2\left(\frac{b_1\,s}{2}\right)\right],\\
T &= \frac{\pi}{2}\left[\frac{\sinh(b_2\,t)}{\tanh(b_2\frac{\pi}{2})}-2\sinh^2\left(\frac{b_2\,t}{2}\right)\right]
\end{aligned}
$$

$$b_1\frac{s_{\max}}{\tanh(b_1 s_{\max})}=b_2\frac{\pi/2}{\tanh(b_2\frac{\pi}{2})},\ \text{with one free parameter.}$$

References

1. L. Laaksonen, P. Pyykkö, D. Sundholm, Comp. Phys. Rept. **4**, 313 (1986).
2. W. Schulze, D. Kolb, Chem. Phys. Lett. **122**, 271 (1985).
3. D. Heinemann, B. Fricke, D. Kolb, Phys. Rev. A **38**, 4998 (1988).
4. D. Heinemann, A. Rosén, B. Fricke, Phys. Scripta **42**, 692 (1990).
5. L. Yang, D. Heinemann, D. Kolb, Chem. Phys. Lett. **178**, 213 (1991).
6. L. Yang, D. Heinemann, D. Kolb, Chem. Phys. Lett. **192**, 499 (1992).
7. L. Yang, D. Heinemann, D. Kolb, Phys. Rev. A **48**, 2700 (1993).
8. C. Düsterhöft, L. Yang, D. Heinemann, D. Kolb, Chem. Phys. Lett. **229**, 667 (1994).
9. C. Düsterhöft, D. Heinemann, D. Kolb, Chem. Phys. Lett. **296**, 77 (1998).
10. O. Kullie, C. Düsterhöft, D. Kolb, Chem. Phys. Lett. **314**, 307 (1999).
11. B. Müller, W. Greiner, Z. Naturf. A **31**, 1 (1976).
12. H. Blum, Q. Lin, R. Rannacher, Numerische Math. **49**, 11 (1986).
13. G. Strange, G. Fix, *An Analysis of the finite Element Methods* (Patric-Hall Inc., Englewood Cliffs) (1973).
14. J.R. Flores, D. Kolb, J. Phys. B **32**, 779 (1999).
15. G. Walz, *Asymptotics and Extrapolation (Berlin Mathematical Research)* (Akademie Verlag, Berlin, 1996), Vol. 88.
16. C. Brezenski, M.R. Zaglai, *Extrapolation Methods. Theory and Practice* (North-Holland, 1991).
17. J. Stoer, R. Bulirsch, *Introduction to Numerical Analysis*, 2nd edn. (Springer Verlag, 1992).
18. A. Rutkowski, Chem. Phys. Lett. **307**, 259 (1999).
19. J. Dolbeault, M.J. Esteban, E. Séré, M. Vanbreugel, Phys. Rev. Lett. **85**, 4020 (2000).
20. A.v. Kopylow, D. Heinemann, D. Kolb, J. Phys. B **31**, 4743 (1998).
21. R. Franke, W. Kutzelnigg, Chem. Phys. Lett. **199**, 561 (1992).
22. R. Franke, Chem. Phys. Lett. **264**, 495 (1997).
23. S.A. Alexander, R.L. Coldwell, Phys. Rev. E **60**, 3374 (1999).
24. F.A. Parpia, A.K. Mohanty, Chem. Phys. Lett. **238**, 209 (1995).
25. L. La John, J.D. Talman, Theo. Chim. Acta **99**, 351 (1998).
26. L. La John, J.D. Talman, Chem. Phys. Lett. **189**, 383 (1992).